Article ID: 1006-8775(2003) 02-0143-09

DCT ANALYSIS DISTRIBUTION FEATURES OF NEAR-SURFACE WIND FIELDS DURING THE LANDFALL OF VONGFONG

LI Jiang-nan (**李江南**)[1] , WANG An-yu (**王安宇**)[1], YANG Zhao-li (**杨兆礼**)[2], LI Guo-li (**李国丽**)[1], WU Chi-sheng (**吴池胜**)[1], HAO I-pan (**侯尔滨**)[3]

(1. *Department of Atmospheric Sciences, Zhongshan University, Guangzhou* 510275 *China*; 2. *Guangzhou Institute of Tropical and Oceanic Meteorology, CMA, Guangzhou* 510080 *China*; 3. *Macao Geophysical and Meteorological Bureau, Macao, China*)

ABSTRACT: Based on the QuikSCAT data, the features of surface wind distribution of the typhoon Vongfong landfall process are analyzed. We have also studied the variance spectral configuration of the surface wind field using DCT (Discrete Cosine Transform). The conclusions are as follows: The near-surface wind field is highly asymmetric; the variance components of asymmetric surface wind field depend mainly on the airflow direction of wavenumber 1 and 2. When the typhoon moves west, there are two wave spectral centers lining up in the zonal direction, mainly the airflow from zonal wavenumber 2 and meridional wavenumber 2; when it moves north, there are two wave spectral centers in a meridional array, mainly the airflow from zonal wavenumber 1 and meridional wavenumber 2. The airflow for wavenumber 1 mainly contributes to the variance of the tangential wind while that for wavenumber 2 to the variance of the radial wind. The asymmetrical distribution changes with the large-scale environment and self-rotating circulation around the typhoon. When it approached land, the associated gale appears in front portion in the advancing direction of the storm. It is in effect similar to the model of Chen Lian-shou for typhoon-related gales —NNW on the left front portion and SE on the right front portion.

Key words: wind distribution; asymmetric; spectral configuration; DCT

CLC number: P457.8 **Document code:** A

1 INTRODUCTION

The typhoon is a destructive weather phenomenon that stands at the top of ten major natural disasters[1]. Typhoon-related damages are the immediate consequences of weather it brings forth, which include heavy rain, strong winds and storm surges (water gain). They cause flash floods, bring down houses and break through dams[1]. Of the research on typhoons for the recent 10 years[2], new advances have been reported on abrupt changes in the motion, structure and intensity of the storm, sudden amplitude increase in the rain it comes with and track forecast. Diagnostic work remains few on the distribution of near-surface (including the sea surface) wind fields around the landfall of typhoons due to limited availability of data concerned. For the purpose, meteorologists and oceanologists usually rely on theoretic and numerical simulations for quantitative discussions[3]. In Liu et al.'s simulations[4], none of the physical fields within the range of the typhoon is symmetric. Blank[5] points out in his harmonic wave study that for the asymmetric outflows from the upper level within the typhoon, most of the variance comes from the air current for wavenumber 1 and 2. With the QuikSCAT satellite data, the current work makes a diagnostic study of Typhoon Vongfong (No.0214) for 2002 in terms of the near-surface

Received date: 2003-06-06; **revised date:** 2003-10-31
Foundation item: Special Fund Project for Social Benefit Research —Study on the Monitoring and Predicting Techniques of Desasters by landding typhoons in China (2002DCA20026-01); Knowledge Innovation Project of The Chinese Academy of Sciences (ZKCXZ-SW-210)
Biography: LI Jiang-nan (1968 –), male, native from Hunan Province, candidate for Ph.D., undertaking the study of numerical simulation and tropical climate.

wind field and strong winds appearance around the point of landfall and discusses its asymmetric spectral configuration using the DCT method.

2 BRIEF ACCOUNT OF MODEL

2.1 *Data*

On August 27th, 1999, a meteorological satellite "QuikSCAT" was launched at NASA. It carried onboard Seawinds, an instrument that is capable of observing wind fields over sea surface (wind speed & direction) at a resolution of 25 km. In contrast to conventional counterparts which can offer only the descriptions of cloud-tops shapes, QuikSCAT gives sea surface wind fields. Many operational meteorological departments use its data to locate the tropical cyclone and estimate the intensity. With the development of the assimilation and retrieval techniques, there have been more and more products based on QuikSCAT data. The products used in the work are provided by COAPS, the Center for Ocean and Atmosphere Prediction Study in Florida, USA, which consists of QuikSCAT data and NCAR/NCEP reanalysis data that are available every 6 hours at a resolution of 0.5°×0.5°. Visit the homepage of COAPS for details. Prior to the study, the data are examined for reliability. They agree well with the observation as far as the track, intensity and maximum wind of the typhoon are concerned. It is a useful attempt to study with the data.

2.2 *The DCT method*

For the diagnostic analysis, the Discrete Consine Transform, DCT, is used to decompose limited-area spectra in 2-dimensional atmospheric fields and the asymmetry of wind fields are discussed in terms of spectral configuration of variance. The DCT method is proposed by Denis et al. recently[6]. Its application is two-folds: One is a quantitative discussion of energy contribution on different scales in limited areas through computation of variance spectra; the other is the filter of two-dimensional fields. Being at the initial phase of application in meteorology, the DCT technique is widely used in the compression of graphic formats of JPEG and MPEG, just like wavelet transform. The latter has become an important tool for spectral analysis of 1-dimensional time series[7]. The following is a brief introduction to the DCT technique.

For a 2-dimensional $N_i \times N_j$ gridpoint field of $f(i, j)$, the conversion and reverse conversion of DCT is shown as

$$F(m, n) = \hat{a}(m)\hat{a}(n) \sum_{i=0}^{i=N_i-1} \sum_{j=0}^{j=N_j-1} f(i, j) \times \cos\left[\pi m \frac{(i+1/2)}{N_i}\right] \cos\left[\pi n \frac{(j+1/2)}{N_j}\right] \tag{1}$$

$$f(i, j) = \sum_{m=0}^{m=N_i-1} \sum_{n=0}^{n=N_j-1} \hat{a}(m)\hat{a}(n) F(m,n) \times \cos\left[\pi m \frac{(i+1/2)}{N_i}\right] \cos\left[\pi n \frac{(j+1/2)}{N_j}\right] \tag{2}$$

in which $\hat{a}(m) = \begin{cases} \sqrt{\frac{1}{N_i}} & m = 0 \\ \sqrt{\frac{2}{N_j}} & m = 1,2,\cdots\cdots,N_j - 1 \end{cases}$, $\hat{a}(n) = \begin{cases} \sqrt{\frac{1}{N_i}} & n = 0 \\ \sqrt{\frac{2}{N_j}} & n = 1,2,\cdots\cdots,N_j - 1 \end{cases}$ (3)

In Eq.(1) – Eq.(3), $f(i, j)$ is the value of meteorological field at the gridpoint (i, j), $F(m,n)$ is the spectral coefficient of the wavenumber (m,n). It is obvious that after transformation, a 2-dimensional $N_i \times N_j$ gridpoint field of $f(i, j)$ will yield a set of $N_i \times N_j$ spectral coefficients $F(m,n)$. The energy spectra of a 2-dimensional meteorological field (to be directly

called variance spectra) can be reflected by means of variance contribution on various scales. Its total variance is expressed as

$$\sigma^2 = \frac{1}{N_i}\frac{1}{N_j}\sum_{i=0}^{i=N_i-1}\sum_{j=0}^{j=N_j-1}\left[f(i,j)-\langle f\rangle\right]^2 \tag{4}$$

in which $\langle f\rangle$ is the mean for the whole region. On the other hand, the total variance is computed through spectral coefficients

$$\sigma^2 = \sum_{\substack{n=0\\(m,n)\neq(0,0)}}^{N_i-1}\sum_{m=0}^{N_j-1}\sigma^2(m,n), \qquad \sigma^2(m,n)=\frac{F^2(m,n)}{N_iN_j} \tag{5}$$

for the regional mean

$$\langle f\rangle = \sqrt{\sigma^2(0,0)} = \frac{F(0,0)}{\sqrt{N_i}\sqrt{N_j}} \tag{6}$$

For a square mesh domain, $N_i = N_j = N$, mesh grid interval is Δ, wavelength is λ, wavenumber is *k*, then

$$l = \frac{2N\Delta}{k} \tag{7}$$

$$k = \sqrt{m^2+n^2} \tag{8}$$

3 FIVE PHASES OF VONGFONG LANDFALL

According to the analysis of Honk Kong Observatory, Typhoon Vongfong (No.0214) evolved to a tropical depression about 280 km SSE of the Xisha Islands on August 15th, 2002. It moved slowly northeast over the initial two days before turning to the NNW. Strengthening to a tropical storm on August 18th, it made recurvature to NNW and got close to the western part of Guangdong coast on August 19th and intensified to a severe tropical storm in the afternoon, with wind force around 25 m/s near the eye. Passing by the northeast coast of Hainan Island, the storm made landfall on Wu Chuan in the night (12:40 L.T.) and weakened rapidly before dissipated over Guangxi.

The variations of the near-surface wind field distribution for Vongfong are what is being discussed in the work, which are available a period from 00:00 August 18th to 06:00 20th (UTC, same below), once every 6 hours and in 10 sets of time level. The time levels contain five stages of the landfall, Stage One from 00:00 to 06:00 August 18 (Levels 1 and 2) when the storm was heading west; Stage Two at 12:00 on the same day (Level 3) when it began to turn right and head north; Stage Three from 18:00 August 18th to 00:"00 August 19th (Levels 4 and 5) when it moved north; Stage Four from 06:00 to 12:00 August 19th (Levels 6 and 7) when it became stronger as it came close to the continent and the pressure was as low as 980 hPa near the center; Stage Five from 18:00 August 19th to 06:00 August 20th (Levels 8, 9, 10) when it landed and dissipated.

4 ASYMMETRIC DISTRIBUTION OF NEAR-SURFACE WIND FIELDS

4.1 *Distribution of asymmetric components*

The asymmetric structure of the typhoon is drawing more and more attention from the meteorologists. As shown in Chen[8] et al. who studied with three target typhoons in the

SPECTRUM-90 experiment, the storms showed asymmetric distribution of isobars before recurvature. Xu and Chen[9] point out that the asymmetricity becomes better-defined after the T42 analysis field was added with intensive soundings and airborne dropsounde data. The typhoon coverage of interest for the work is shown in Fig.1, which is a circle that takes the eye as the origin and is 1000 km on the radius. The original rectangular _ Z coordinates (x, y, z) is changed to the cylindrical _ Z coordinates (r, q, z). To have better discussion of the asymmetric near-surface wind fields,

$$V_m = \frac{\int_0^{2\delta} \int_{r_0}^{r_0+\Delta r} V dr d\theta}{\int_0^{2\delta} \int_{r_0}^{r_0+\Delta r} r dr d\theta}, V' = V - V_m \tag{9}$$

is defined. The equation has the physical meaning that the symmetric components are separated from the asymmetric ones for the near-surface wind field within the domain of the typhoon. r_0 is the initial radius of the integration, taking 0, 100, 200, 300, 400, 500, 600, 700, 800 and 900 km, respectively, with $\Delta r = 100$ km. V is the value of the gridpoint field within the radial range of integration. It is obvious that V_m is a symmetric component while V' is a asymmetric one.

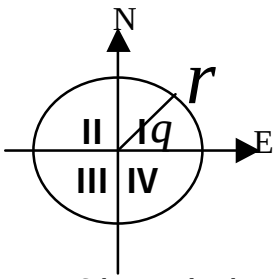

Fig.1 Schematic distribution of typhoon quadrants

Fig.2 gives the distribution of isolines of asymmetric components in the near-surface wind field (total wind speed) within the typhoon range in the five stages of landfall (at Levels 1, 3, 5, 7 and 9) at intervals of 2 m/s. It shows clear asymmetry in the wind field for all of the stages, though with different characteristics from stage to stage. In Stage One, there were three positive and three negative anomalous areas as the typhoon moved west, with the maximum anomalous center in the northeast. As shown in the flow field at 850 hPa and 500 hPa (figure omitted), it was resulted from convergence of the easterly, the steering air current south of the storm, with the cyclonic circulation rotating around it. In Stage Two, the typhoon track turned right and northward with only two positive and two negative anomalous areas left. The original maximum anomalous area disappeared, a sign that strong southwesterly spirals in from south of the typhoon as it moved west and the asymmetric low-level flow field could provide the typhoon system with the energy it needed to converge northward to cause the storm to slow down and turn right and north. The fact agrees with Yang's theoretic analysis[10] who works on the role of non-linear momentum advection on track recurvature of typhoons. In Stage Three, the typhoon kept heading NWN continuously subject to the subtropical high, with a large area of positive anomalies and a large area of negative anomalies, each in a semi-circle aligning up SW —NE on the radial line, in which the right semi-sphere into which the steering airflow made its entrainment is the positive anomalous area. About 500 km southwest of the eye there was a center of strong winds with dense distribution of isolines. As shown in the flow field at 850 hPa (figure omitted), it was caused by superimposition of a southerly jet with the cyclonic circulation. In Stage Four, the typhoon got close to the continent and intensified, with similar distribution of positive and negative anomalies over extensive regions as Stage Three. The difference was that the center of strong winds had disappeared south of the typhoon. Two new centers of strong winds formed on the coastline ahead of the eye on both sides of the Leizhou Peninsula. In Stage Five, the wind speed decreased rapidly, the isolines got less dense and airflow was much stronger in the rear than in the front of the typhoon. In brief, the asymmetry is obvious in the wind field near the surface during the landfall.

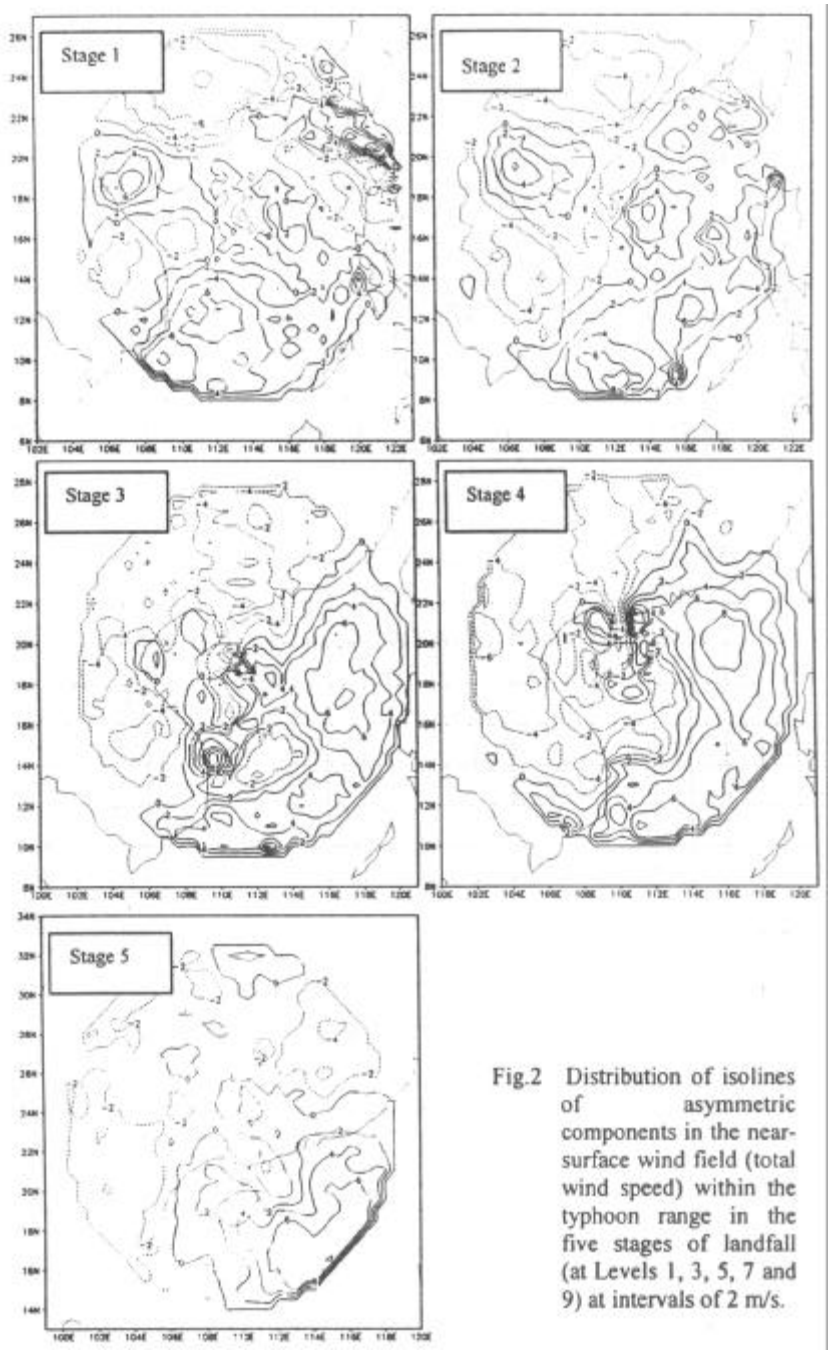

Fig.2 Distribution of isolines of asymmetric components in the near-surface wind field (total wind speed) within the typhoon range in the five stages of landfall (at Levels 1, 3, 5, 7 and 9) at intervals of 2 m/s.

4.2 *Distribution of strong winds around landfall*

As early as in the 1970' s, Chen and Ding divided the appearance of gale around the point of landfall into two types and Vongfong' s wind field evolution during the landfall was similar to the strong wind model in Category Two typhoons. Fig.3 gives the wind field vector and distribution of isolines for wind speeds larger than Force 6 (10.7 m/s). From the figure, we know that two new centers of gale form in the front of the eye, with southeasterly in the right front portion and NWN wind in the left front portion.

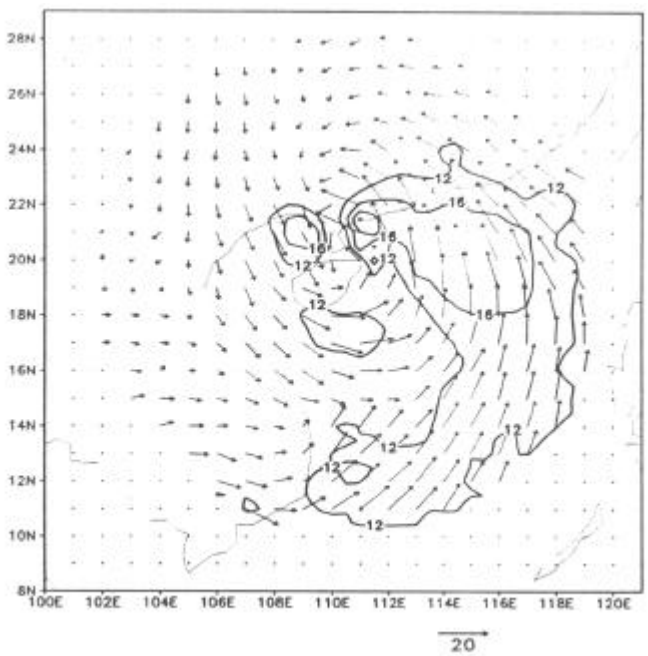

Fig.3 Wind field vector and distribution of isolines for wind speeds larger than Force 6 (10.7 m/s).

5 WAVE CONFIGURATION STRUCTURE OF ASYMMETRIC WIND FIELD NEAR THE SURFACE

As shown in the study above, asymmetric features are obvious in the distribution of near-surface wind field of the typhoon, which agrees well with the results of Liu et al. [5] in their numerical study. With harmonic analysis, Bland et al. point out that most of the variance come from the airflow with wavenumber 1 and 2 for the asymmetric outflowing current from the upper level within the range of the typhoon. What are the characteristics of the wave configuration structure then? For the purpose, we selected a square domain with 40×40 gridpoints to conduct a DCT study, in which the typhoon center is the center of the square.

Fig.4 gives the contribution by variance of airflow with different wavenumber for Stage One (Those with the wavenumber above 20 have been removed for clear graphic display). The variance for the asymmetric near-surface wind field is mostly contributed by airflow with wavenumber 1 and 2, as in the previous case, though the radial wind differs much with the tangential wind. Airflow of wavenumber 1 mainly contributes to the variance of the tangential wind while that of wavenumber 2 mainly contributes to the variance of the radial wind. In addition to disturbances from large-scale airflow of wavenumber 1 and 2, there are also disturbances resulting from relatively smaller mesoscale airflow. Situations are similar for the other stages and will not elaborated here to save text.

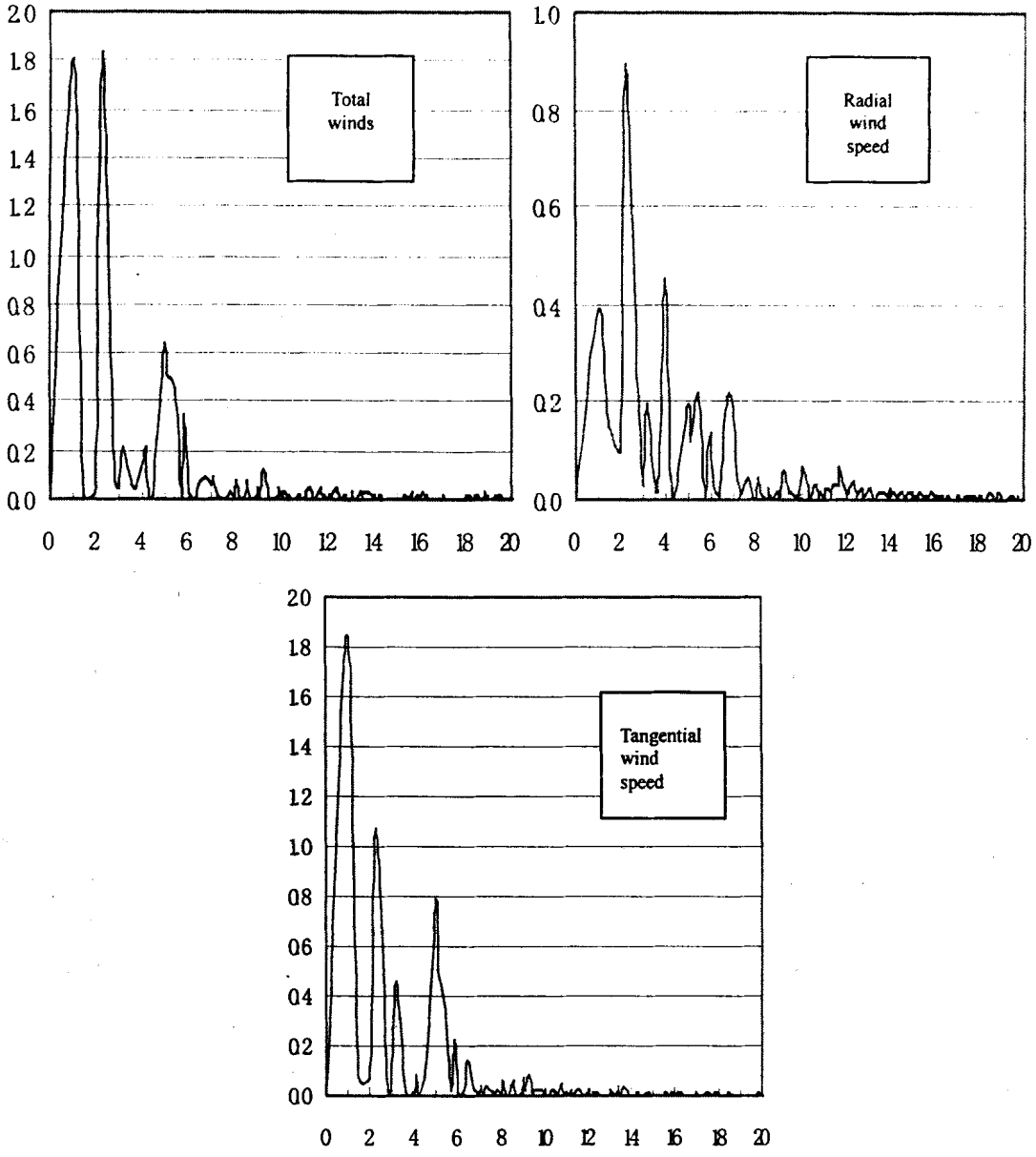

Fig.4 Contribution by variance of airflow with different wavenumber for Stage One. The ordinate is the variance in unit of m^2/s^2 and the abscissa is the wavenumber *k*.

Fig.5 gives the structure of variance spectra for the near-surface wind field (total wind speed) within the typhoon range over the five stages of landfall (on the 1st, 3rd, 5th, 7th and 9th time levels, respectively). The figure shows that the variance of the wind field is not only related with the number of wavenumber but also with the direction of the wave. The relation shows with the changes in the direction in which the typhoon is moving. In Stage One, the typhoon moved west, with two zonally-positioning centers of wave configuration, mainly consisting of airflow with zonal wavenumber 2 and meridional wavenumber 1. In Stage Two, the wave configuration became more complicated as the recurvature occurred so that the centers began to turn from

zonal alignment to meridional alignment, suggesting major effect of an adjusted large-scale environment field on the track of the typhoon. In Stage Three, the typhoon moved north on the meridional circle, with two centers of wave configuration meridionally positioned, mainly consisting of airflow with zonal wavenumber 1 and meridional wavenumber 2. It is just the opposite with the case in Stage One. In Stage Four, the distribution is more obvious with denser isolines and increased asymmetry. In Stage Five, the total variance decreased as the typhoon weakened rapidly and the isolines got less dense.

In summary, the variance of asymmetric wind fields near the surface within the range of the typhoon is mostly from airflow with wavenumber 1 and 2. It is not only related to the size of the wavenumber but also with its direction. The relationship is displayed as the typhoon changes the direction of motion.

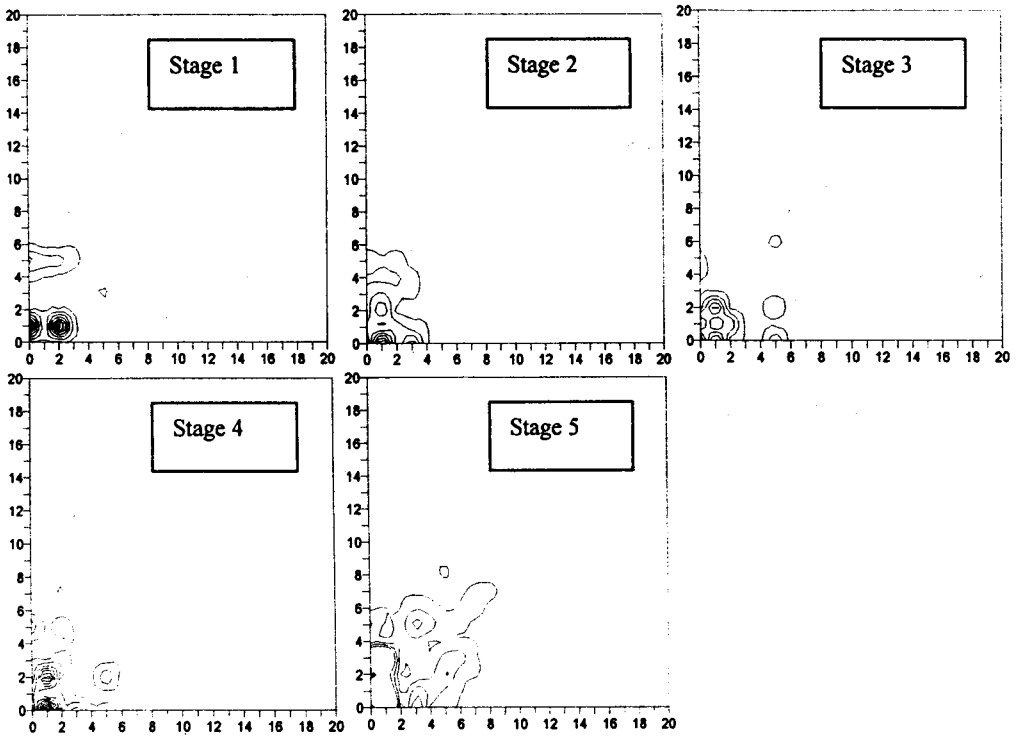

Fig.5 Structure of variance spectra for the near-surface wind field (total wind speed) within the typhoon range. The abscissa is the zonal wavenumber *m*, the ordinates is the meridional wavenumber *n* and the interval of isolines is $0.2\,m^2/s^2$.

6 CONCLUSIONS AND DISCUSSIONS

a. The near-surface wind field of typhoons is clearly asymmetric, which changes as the ambient and cyclonic circulation rotating around the storm. More is to be done to study the complicated causation for the asymmetric wind field —does it have anything to do with terrain or does it result from structural changes in the evolution of the typhoon, or is it a consequence from the joint effect of both factors?

b. The variance of the asymmetric wind field near the surface within the typhoon influence is mostly from airflow with wavenumber 1 and 2 and it is related with the direction of the wave. When the typhoon moves west, there are two zonally-positioning centers of wave configuration, mainly consisting of airflow with zonal wavenumber 2 and meridional wavenumber 1. The

airflow of wavenumber 1 contributes the most to the variance of the tangential wind while that of wavenumber 2 to the variance of the radial wind.

c. Typhoon-affiliated strong winds appear in the front portion in front of it when it moves close to the continent and the intensity rapidly decreases after landfall. It is similar to the model of Category Two of strong winds, which is summarized by Chen and Ding[2] —the NNW wind is found on the left front portion and SE on the right front portion.

The work utilizes the latest source of observations and updated technique of diagnosis, which proves a useful attempt. Plenty of justification needs to be done for the conclusions drawn from the single case of Vongfong. More work is to continue on the characteristics of the near-surface wind field with varying track, ambient fields or underlying surface.

Acknowledgements: Mr. CAO Chao-xiong, who works at the Institute of Tropical and Marine Meteorology, CMA, Guangzhou, has translated the paper into English.

REFERENCES:

[1] CHEN Lian-shou, DING Yi-hui. General Introduction of Typhoons in West Pacific [M]. Beijing: Science Press, 1979, 440.
[2] CHEN Lian-shou, MENG Zhi-yong. Ten-year advances in the research on tropical cyclones in China [J]. *Chinese Journal of Atmospheric Sciences*, 2001, **25**: 420-432.
[3] MA Yang, ZHANG Qing-hua. Discussion on some issues of advances in typhoon wind fields [J]. *Journal of Oceanography of Huanghai & Bohai Seas*, 1999, **17**: 61-64.
[4] LIU Y, ZHANG D L, YAU M K. A multiscale numerical study of hurricane and Rew (1992). Part I: Explicit simulation and verification [J]. *Monthly Weather Review*, 1999, **125**: 3073-3093.
[5] BLACK, ANTHES R A. On the asymmetric structure of the tropical cyclone outflow layer[J]. *Journal of Atmospheric Science*, 1971, **28**: 1348-1366.
[6] DENIS B, COTE J, LAPRISE R. Spectral decomposition of two-dimensional atmospheric fields on limited-area domains using the Discrete Consine Transform (DCT) [J]. *Monthly Weather Review*, 2002, **130**: 1812-1829.
[7] LI Jiang-nan, MENG Wei-guang, WANG An-yu, et al. Climatological characteristics of intensity and location of the subtropical high in western Pacific [J]. *Tropical Geography*, 2003, **23**: 35-39.
[8] CHEN Lian-shou, LUO Zhen-xian. Some relations between asymmetric structure and motion of typhoons [J]. *Acta Meteorologica Sinica*, 1995, **9**: 412-419.
[9] XU Xiang-de, CHEN Lian-shou. Characteristics of asymmetric structure of peg-top "ventilation flow" in the target experimental Typhoon Flo during TCM-90 [J]. *Acta Meteorologica Sinica*, 1996, **54**: 536-543.
[10] YANG Pingzhang, HE Hai-yan. Effects of non-linear horizontal momentum advection on tropical cyclone advection [J]. *Acta Scientiarum Naturalium Univesitatis Sunyatseni*, 1995, **34**: 82-89.